

# A Fast Algorithm for Simulating the Chordal Schramm-Loewner Evolution

Tom Kennedy  
Department of Mathematics  
University of Arizona  
Tucson, AZ 85721  
<http://www.math.arizona.edu/~tgk>  
email: [tgk@math.arizona.edu](mailto:tgk@math.arizona.edu)

September 9, 2018

## Abstract

The Schramm-Loewner evolution (SLE) can be simulated by dividing the time interval into  $N$  subintervals and approximating the random conformal map of the SLE by the composition of  $N$  random, but relatively simple, conformal maps. In the usual implementation the time required to compute a single point on the SLE curve is  $O(N)$ . We give an algorithm for which the time to compute a single point is  $O(N^p)$  with  $p < 1$ . Simulations with  $\kappa = 8/3$  and  $\kappa = 6$  both give a value of  $p$  of approximately 0.4.

# 1 Introduction

The Schramm-Loewner evolution (SLE) is a stochastic process that produces a random curve in the complex plane. In this paper we will be concerned with chordal SLE in which the random curve, the SLE “trace,” lies in the upper half plane and goes from 0 to  $\infty$ . The classical Loewner equation is

$$\partial_t g_t(z) = \frac{2}{g_t(z) - U_t} \tag{1}$$

with the initial condition  $g_0(z) = z$ . Here  $U_t$  is a real-valued “driving function.” The equation defines a one parameter family  $g_t$  of conformal maps from a simply connected subset of the upper half plane onto the upper half plane. SLE is obtained by taking  $U_t = \sqrt{\kappa}B_t$  where  $\kappa > 0$  is a parameter and  $B_t$  is a Brownian motion with mean zero and variance  $t$ . For further discussion of SLE we refer the reader to [7, 10] and the original references [8, 9].

The most common method for simulating SLE is not to numerically solve the above differential equation. Instead one partitions the time interval into  $N$  subintervals and approximates  $g_t$  by the composition of a sequence of  $N$  conformal maps which are approximations to the solution of the Loewner equation over the subintervals. Computing a point on the SLE trace requires evaluating the composition of roughly  $N$  conformal maps and so takes a time  $O(N)$ . We will refer to the time it takes to compute one point on the SLE trace as the “time per point.”

The goal of this paper is to give an algorithm for which the time per point is  $O(N^p)$  with  $p < 1$ . We do not prove that our algorithm does this. The time our algorithm takes to generate an SLE curve depends on the behavior of the particular curve. For certain atypical curves, our algorithm will not be faster than the usual algorithm. So a rigorous analysis of our algorithm is a daunting task. We have studied the behavior of the algorithm by simulation for  $\kappa = 8/3$  and  $\kappa = 6$ . For both of these values of  $\kappa$ , the time per point for our algorithm is  $O(N^p)$  with  $p$  around 0.4. Figures 1 and 2 show log-log plots of the time per point as a function of  $N$  for the usual algorithm and for our new algorithm. In the first figure  $\kappa = 8/3$ , and in the second it is 6. Although the behavior of the SLE trace is qualitatively different for these two values of  $\kappa$ , the behavior of the time required for the simulation is quite similar. The straight lines show fits by  $c_1N$  for the usual algorithm and by  $c_2N^{0.4}$  for our algorithm. For  $N = 100,000$  our algorithm is faster by approximately a factor of 14 and for  $N = 1,000,000$  our algorithm is faster by approximately a factor of 56.

There is an inverse problem that is closely related to the present paper. Given a simple curve in the upper half plane, compute the corresponding driving function in the Loewner equation. An important application of this inverse problem is studying if a family of random curves is SLE. Given a large sample of the curves, one computes the corresponding samples of the driving function and then tests if they are a Brownian motion. This was done for interfaces in two-dimensional spin glass ground states in [1, 5] and for certain isolines in two-dimensional models of turbulence in [3, 4]. The methods of this paper apply to this inverse problem as well. The naive implementation of the zipper algorithm to compute the driving function for a curve

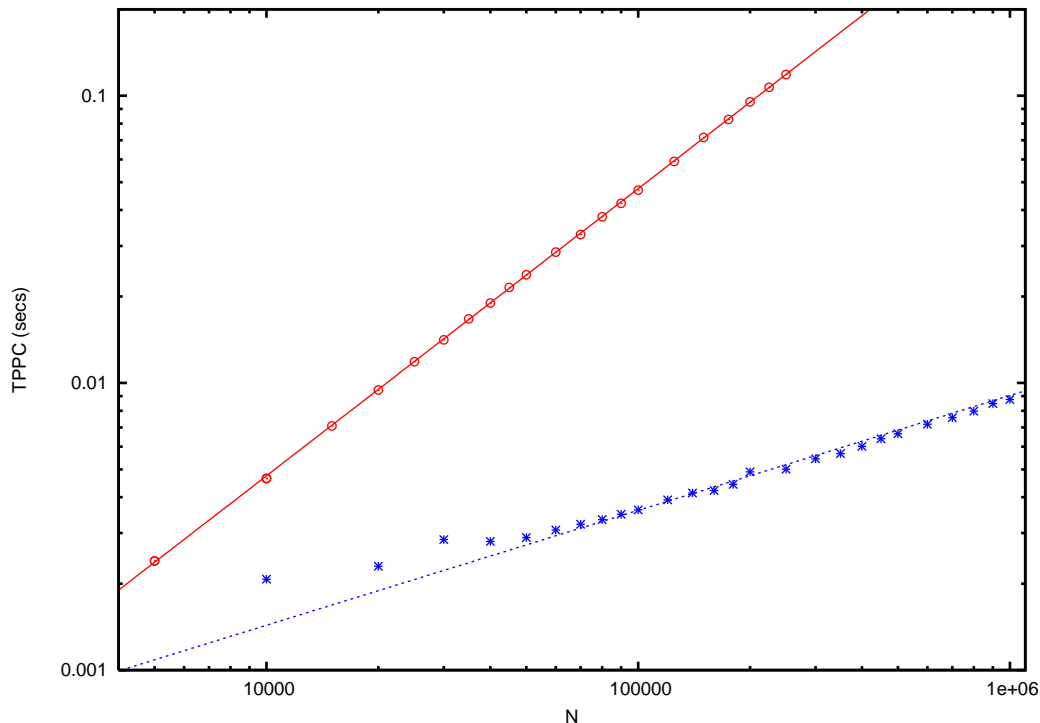


Figure 1: Time per point computed as a function of  $N$ , the number of subintervals in the partition of the time interval for  $\kappa = 8/3$ . The top curve is the usual algorithm; the bottom curve is the new algorithm. The lines shown have slopes 1 and 0.4.

with  $N$  points runs in a time  $O(N^2)$ . Using the methods of this paper, the algorithm runs in a time  $O(N^{1.35})$ . This fast algorithm is studied in [6].

In section 2 we explain the standard method for “discretizing” SLE. A particular example was studied by Bauer [2]. The material in this section is well known but does not seem to have appeared in the literature yet. In section 3 we explain our new algorithm. The algorithm involves several parameters, so in section 4 we study how the error and time required for the algorithm depend on these parameters. The appendix gives some power series needed in particular implementations of the algorithm. C++ code implementing the new algorithm may be downloaded from the author’s homepage.

## 2 Discretizing SLE

We are going to approximate SLE by a “discrete SLE.” The term discrete SLE is a bit misleading. The random process we define produces continuous curves in the upper half plane. The plane is not replaced by a lattice. Let  $0 = t_0 < t_1 < t_2 < \dots < t_n = 1$  be a partition of the time interval  $[0, t]$ . (Thanks to the scaling property of SLE, it is no loss of generality to

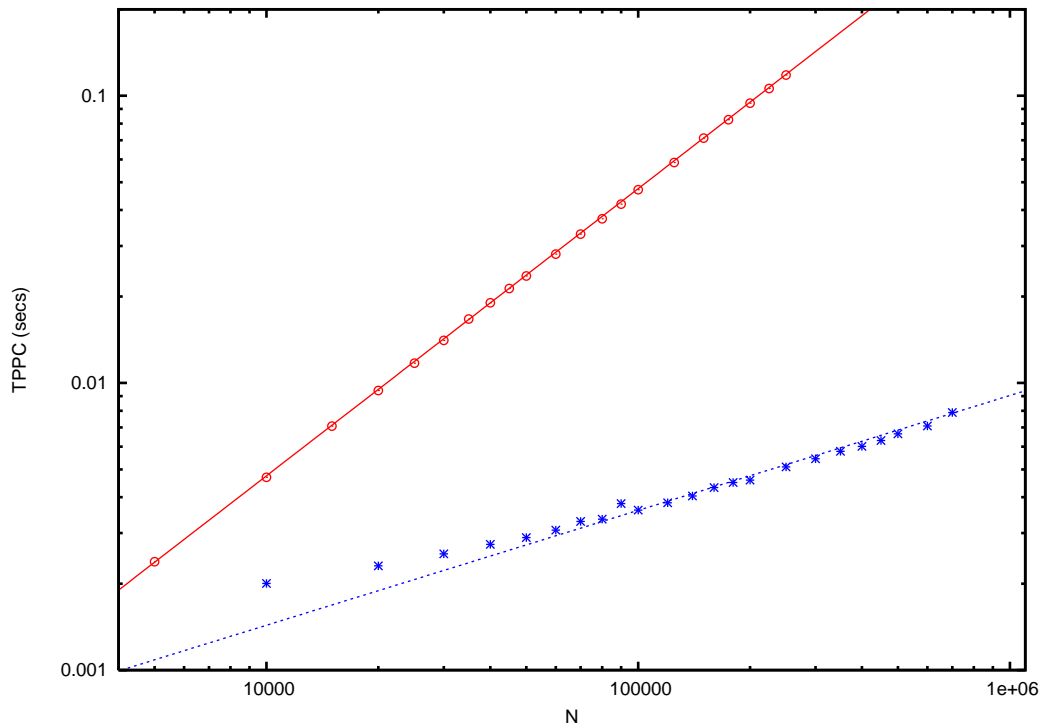


Figure 2: Time per point computed as a function of  $N$ , the number of subintervals in the partition of the time interval for  $\kappa = 6$ . The lines shown have slopes 1 and 0.4.

take the time interval to be  $[0, 1]$ .) The times  $t_k$  play a special role, but the random curves are still defined for all time. We can think of our discrete approximation as the result of replacing the Brownian motion in the driving function by some stochastic process that approximates (or even equals) the Brownian motion at the times  $t_k$ , and is defined in between these times so that the Loewner equation may be solved explicitly.

We begin by reviewing some facts about the Schramm-Loewner evolution for the upper half-plane,

$$\partial_t g_t(z) = \frac{2}{g_t(z) - \sqrt{\kappa}B_t} \quad (2)$$

with  $g_0(z) = z$ . The set  $K_t$  contains the points  $z$  in the upper half-plane for which the solution to this equation no longer exists at time  $t$ . Let  $t, s > 0$ . The map  $g_{t+s}$  maps  $\mathbb{H} \setminus K_{t+s}$  onto  $\mathbb{H}$ . We can do this in two stages. We first apply the map  $g_s$ . This maps  $\mathbb{H} \setminus K_s$  onto  $\mathbb{H}$ , and it maps  $\mathbb{H} \setminus K_{t+s}$  onto  $\mathbb{H} \setminus g_s(K_{t+s} \setminus K_s)$ . Let  $\hat{g}_t$  be the conformal map that maps  $\mathbb{H} \setminus g_s(K_{t+s} \setminus K_s)$  onto  $\mathbb{H}$  with the usual hydrodynamic normalization. By the uniqueness of these maps,

$$g_{s+t} = \hat{g}_t \circ g_s, \quad i.e., \quad \hat{g}_t = g_{s+t} \circ g_s^{-1} \quad (3)$$

Then

$$\frac{d}{dt}\hat{g}_t(z) = \frac{d}{dt}g_{s+t} \circ g_s^{-1}(z) = \frac{2}{g_{s+t} \circ g_s^{-1}(z) - U_{s+t}} = \frac{2}{\hat{g}_t(z) - U_{s+t}} \quad (4)$$

Note that  $\hat{g}_0(z) = z$ . Thus  $\hat{g}_t(z)$  is obtained by solving the Loewner equation with driving function  $\hat{U}_t = U_{s+t}$ . This driving function starts at  $U_s$ , and so the  $\hat{K}_t$  associated with  $\hat{g}_t$  starts growing at  $U_s$ . In our approximation the driving function will be sufficiently nice that  $\hat{K}_t$  is just a curve which starts at  $U_s$ .

We now return to the partition  $0 = t_0 < t_1 < t_2 < \dots < t_n = 1$ , and define

$$G_k = g_{t_k} \circ g_{t_{k-1}}^{-1} \quad (5)$$

So

$$g_{t_k} = G_k \circ G_{k-1} \circ G_{k-2} \circ \dots \circ G_2 \circ G_1 \quad (6)$$

By the remarks above,  $G_k(z)$  is obtained by solving the Loewner equation with driving function  $U_{t_{k-1}+t}$  for  $t = 0$  to  $t = \Delta_k$ , where  $\Delta_k = t_k - t_{k-1}$ . Note that  $G_k$  maps  $\mathbb{H}$  minus a set “centered” around  $U_{t_{k-1}}$  to  $\mathbb{H}$ . If we consider  $G_k(z + U_{t_{k-1}+t}) - U_{t_{k-1}}$ , it is obtained by solving the Loewner equation with driving function  $U_{t_{k-1}+t} - U_{t_{k-1}}$  for  $t = 0$  to  $t = \Delta_k$ . This driving function starts at 0 and ends at  $\delta_k$  where  $\delta_k = U_{t_k} - U_{t_{k-1}}$ . So this conformal map takes  $\mathbb{H}$  minus a set “centered” around the origin onto  $\mathbb{H}$ .

The approximation to the SLE trace is given by  $\gamma(t) = g_t^{-1}(U_t)$ . Let  $z_k = g_{t_k}^{-1}(U_{t_k})$ . We will only consider the points on this curve which correspond to times  $t = t_k$ . One could consider other points on the curve, but the distance between consecutive  $z_k$  is already of the order of the error in our approximation, so there is little reason to consider more points. The points  $z_k$  are given by

$$z_k = G_1^{-1} \circ G_2^{-1} \circ \dots \circ G_{k-1}^{-1} \circ G_k^{-1}(U_{t_k}) \quad (7)$$

We would like to rewrite this using conformal maps that depend only on the change in  $U_t$  over the time intervals. Define

$$h_k(z) = G_k^{-1}(z + U_{t_k}) - U_{t_{k-1}} \quad (8)$$

So

$$z_k = h_1 \circ h_2 \circ \dots \circ h_{k-1} \circ h_k(0) \quad (9)$$

Recall that if we solve the Loewner equation with driving function  $U_{t_{k-1}+t} - U_{t_{k-1}}$  for  $t = 0$  to  $t = \Delta_k$ , we get  $g_k(z)$  where

$$g_k(z) = G_k(z + U_{t_{k-1}}) - U_{t_{k-1}} \quad (10)$$

Letting  $f_k(z) = g_k^{-1}(z)$ , we have

$$f_k(z) = G_k^{-1}(z + U_{t_{k-1}}) - U_{t_{k-1}} \quad (11)$$

and so  $h_k(z) = f_k(z + \delta_k)$ . As noted above,  $f_k$  maps  $\mathbb{H}$  to  $\mathbb{H}$  minus a curve that starts at 0. The driving function ends at  $\delta_k$ , so  $f_k(\delta_k)$  is the tip of the curve. It follows that  $h_k(z)$  maps  $\mathbb{H}$  onto  $\mathbb{H}$  minus a curve starting at 0 and  $h_k(0)$  is the tip of the curve. Thus we have the following

simple picture for eq. (9). The first map  $h_k$  welds together a small interval on the real axis containing the origin to produce a small cut. The origin is mapped to the tip of this cut. The second map welds together a (possibly different) small interval in such a way that it produces another small cut. The original cut is moved away from the origin with its base being at the tip of the new cut. This process continues. Each map introduces a new small cut whose tip is attached to the image of the base of the previous cut.

The key idea is to define  $U_t$  for  $t_{k-1} \leq t \leq t_k$  so that  $g_k(z)$  may be explicitly computed. There are two constraints on  $g_k$ . The curve must have capacity  $2\Delta_k$  and  $g_k$  must map the tip of the curve to  $\delta_k$ . Given any simple curve satisfying these two constraints and starting at the origin, it will be the solution of the Loewner equation for some driving function which goes from 0 to  $\delta_k$  over the time interval  $[0, \Delta_k]$ . Different choices of this interpolating curve give us different discretizations. Before we discuss particular discretizations, we will discuss the definitions of  $\Delta_k$  and  $\delta_k$ .

The simplest choice for  $\Delta_k$  is to use a uniform partition of the time interval,  $\Delta_k = 1/N$ . However, if we use a uniform partition and look at the resulting points  $z_k$ , they appear to be farther apart on average at the beginning of the curve than at the end. To understand this, consider the case of  $\kappa = 8/3$  which is believed to correspond to the self-avoiding walk. Let  $\omega(s)$  denote the scaling limit of the self-avoiding walk. With its natural parameterization we have  $E\omega(s)^2 = cs^{2\nu}$  where  $\nu = 3/4$  and  $c$  is a constant. If we take points at equally spaced times using this parameterization we will get points on the walk that are roughly equally distant. For *SLE* with its parameterization using capacity, we have  $E\omega(t)^2 = ct$  for some constant  $c$ . To match these two parameterizations in an average sense we should take  $t = s^{2\nu}$ . Thus to get points approximately equally spaced on the SLE curve, we should take  $t_k = (k/N)^{2\nu}$ .

The  $\delta_k$  should be chosen so that the stochastic process  $U_t$  will converge to  $\sqrt{\kappa}$  times Brownian motion as  $N \rightarrow \infty$ . One possibility is take the  $\delta_k$  to be independent normal random variables with mean zero and variance  $\kappa\Delta_k$ . If we do this, then  $U_t$  and  $\sqrt{\kappa}B_t$  will have the same distributions if we only consider times chosen from the  $t_k$ . Another possibility is to take the  $\delta_k$  to be independent random variables with  $\delta_k = \pm\sqrt{\kappa\Delta_k}$  where the choices of  $+$  and  $-$  are equally probable. If we use this choice with the uniform partition of the time interval, then we are approximating the Brownian motion by a simple random walk.

We now consider specific choices of the interpolating curve used for the discretization. A popular choice is the following. Let  $C$  be a line segment starting at the origin with a polar angle of  $\alpha\pi$ .  $g_k$  maps  $\mathbb{H} \setminus C$  onto  $\mathbb{H}$ . There are two degrees of freedom for the line segment - its length and  $\alpha$ . There are two constraints - the line segment must have capacity  $2\Delta_k$  and the tip of the segment must get mapped to  $\delta_k$ .

Consider the map

$$\phi(z) = (z + y)^{1-\alpha}(z - x)^\alpha \tag{12}$$

where  $x, y > 0$ . It maps the half plane onto the half plane minus a line segment which starts at the origin and forms an angle  $\alpha$  with the positive real axis. The interval  $[-y, x]$  gets mapped onto the slit. The length of this interval determines the length of the slit. Shifting this interval (relative to 0) does not change the length of the slit. To obtain the map  $g_k$ , we must choose  $x$

and  $y$  so that  $g_k$  satisfies the hydrodynamic normalization and has capacity  $2\Delta_k$ . Tedious but straightforward calculation shows if we let

$$f_t(z) = \left( z + 2\sqrt{t}\sqrt{\frac{\alpha}{1-\alpha}} \right)^{1-\alpha} \left( z - 2\sqrt{t}\sqrt{\frac{1-\alpha}{\alpha}} \right)^\alpha \quad (13)$$

then  $f_t^{-1}(z)$  satisfies the hydrodynamic normalization and has capacity  $2t$ . In particular,  $f_k(z)$  is given by the above equation with  $t = \Delta_k$ . We know from the general theory that  $g_t(z) = f_t^{-1}(z)$  satisfies the Loewner equation (1) for some driving function  $U_t$ . Some calculation then shows that

$$U_t = c_\alpha \sqrt{t} \quad (14)$$

where

$$c_\alpha = 2 \frac{1-2\alpha}{\sqrt{\alpha(1-\alpha)}} \quad (15)$$

For the map  $g_k$  we need  $U_{t_k} - U_{t_{k-1}} = \delta_k$ , and so

$$\delta_k = c_\alpha \sqrt{\Delta_k} \quad (16)$$

This equation determines  $\alpha$ . ( $\alpha$  depends on  $k$ .)

Define

$$v = \frac{\delta_k^2}{\Delta_k} \quad (17)$$

Then squaring (16) gives

$$c_\alpha^2 = v \quad (18)$$

which leads to

$$16\alpha^2 + v\alpha^2 - 16\alpha - v\alpha + 4 = 0 \quad (19)$$

and so

$$\alpha = \frac{1}{2} \pm \frac{1}{2} \sqrt{\frac{v}{16+v}} \quad (20)$$

We take the choice with  $\alpha < 1/2$  if  $\delta_k > 0$  and the choice with  $\alpha > 1/2$  if  $\delta_k < 0$ . Using  $h_k(z) = f_k(z + \delta_k)$  we find that

$$h_k(z) = \left( z + 2\sqrt{\frac{\Delta_k(1-\alpha)}{\alpha}} \right)^{1-\alpha} \left( z - 2\sqrt{\frac{\Delta_k\alpha}{1-\alpha}} \right)^\alpha \quad (21)$$

Note how confusingly similar this formula is to (13).

Another discretization is to take

$$h_k(z) = \sqrt{z^2 - 4\Delta_k} + \delta_k \quad (22)$$

This conformal map produces a vertical slit based at  $\delta_k$  with capacity  $2\Delta_k$ . It does not map the origin to the tip of the slit. So composing these maps does not produce a curve. Nonetheless, this discretization converges to SLE [2]. A vertical slit corresponds to a constant driving function. So this discretization corresponds to replacing the Brownian motion by a stochastic process that is constant on each time subinterval and jumps discontinuously at the times  $t_k$ .

### 3 A faster algorithm

To motivate what we do in this section, we first consider the speed of the algorithm described in the previous section. Recall that points on the approximation to the SLE trace are given by

$$z_k = h_1 \circ h_2 \circ \cdots \circ h_{k-1} \circ h_k(0) \tag{23}$$

The number of operations needed to compute a single  $z_k$  is proportional to  $k$ . So to compute all the points  $z_k$  with  $k = 1, 2, \dots, N$  requires a time  $O(N^2)$ .

It is important to note that the computation of  $z_k$  does not depend on any of the other  $z_j$ . So we can compute a subset of the points  $z_k$  if we desire. (As an extreme example, if we are only interested in  $z_N = \gamma(1)$ , the time required for the computation is  $O(N)$  not  $O(N^2)$ .) For the timing tests in this paper we compute the points  $z_{jd}$  with  $j = 1, 2, \dots, N/d$  where  $d$  is some integer. But we emphasize that our algorithm works for any choice of the set of points to compute. For the above algorithm the time grows as  $N^2/d$ . The time per point grows as  $N$ . We use the time per point throughout this paper to study the efficiency. It is a natural measure since it depends on how finely we discretize the time interval but not on the number of points we choose to compute. The total time to compute the SLE trace is given by the number of points we want to compute on it times the time per point. Our goal is to develop an algorithm for which the time per point is  $O(N^p)$  with  $p < 1$ .

Our algorithm begins by grouping the functions in (23) into blocks. The number of functions in a block will be denoted by  $b$ . Let

$$H_j = h_{(j-1)b+1} \circ h_{(j-1)b+2} \circ \cdots \circ h_{jb} \tag{24}$$

If we write  $k$  as  $k = mb + l$  with  $0 \leq l < b$ , then we have

$$z_k = H_1 \circ H_2 \circ \cdots \circ H_m \circ h_{mb+1} \circ h_{mb+2} \circ \cdots \circ h_{mb+l}(0) \tag{25}$$

The number of compositions in (25) is smaller than the number in (23) by roughly a factor of  $b$ . Unfortunately, even though the  $h_i$  are relatively simple, the  $H_j$  cannot be explicitly computed. Our strategy is to approximate the  $h_i$  by functions whose compositions can be explicitly computed to give an explicit approximation to  $H_j$ . For large  $z$ ,  $h_i(z)$  is well approximated by its Laurent series about  $\infty$ . One could approximate  $h_i$  by truncating this Laurent series. This is the spirit of our approach, but our approximation is slightly different.

Let  $f(z)$  be a conformal map from  $\mathbb{H}$  onto  $\mathbb{H} \setminus \gamma[0, t]$ , where  $\gamma : [0, t] \rightarrow \mathbb{H}$  is a curve in the upper half plane with  $\gamma(0) = 0$ . We assume that  $f(\infty) = \infty$ ,  $f'(\infty) = \infty$  and  $f(0) = \gamma(t)$ . Let



$a, b > 0$  be such that  $[-a, b]$  is mapped onto the slit  $\gamma[0, t]$ . So  $f$  is real valued on  $(-\infty, -a]$  and  $[b, \infty)$ . By the Schwartz reflection principle,  $f$  has an analytic continuation to  $\mathbb{C} \setminus [-a, b]$ , which we will simply denote by  $f$ . Let  $R = \max\{a, b\}$ , so  $f$  is analytic on  $\{z : |z| > R\}$  and maps  $\infty$  to itself. Thus  $f(1/z)$  is analytic on  $\{z : 0 < |z| < 1/R\}$  and our assumptions on  $f$  imply it has a simple pole at the origin with residue 1. So we have

$$f(1/z) = 1/z + \sum_{k=0}^{\infty} c_k z^k \quad (26)$$

This gives the Laurent series of  $f$  about  $\infty$ .

$$f(z) = z + \sum_{k=0}^{\infty} c_k z^{-k} \quad (27)$$

If we truncate this Laurent series, it will be a good approximation to  $f$  for large  $z$ . At first sight, this Laurent series is the natural approximation to use for  $f$ . However, we will use a different but closely related representation.

Define  $\hat{f}(z) = 1/f(1/z)$ . Since  $f(z)$  does not vanish on  $\{|z| > R\}$ ,  $\hat{f}(z)$  is analytic in  $\{z : |z| < 1/R\}$ . Our assumptions on  $f$  imply that  $\hat{f}(0) = 0$  and  $\hat{f}'(0) = 1$ . So  $\hat{f}$  has a power series of the form

$$\hat{f}(z) = \sum_{j=0}^{\infty} a_j z^j \quad (28)$$

with  $a_0 = 0$  and  $a_1 = 1$ . It is not hard to show that  $1/R$  is the radius of convergence of this power series. We will refer to this power series as the “hat power series” of  $f$ . Note that the coefficients of the hat power series of  $f$  are the coefficients of the Laurent series of  $1/f$ .

The primary advantage of this hat power series over the Laurent series is its behavior with respect to composition.

$$(f \circ g)^\wedge(z) = 1/f(1/\hat{g}(z)) = \hat{f}(\hat{g}(z)) \quad (29)$$

Thus

$$(f \circ g)^\wedge = \hat{f} \circ \hat{g} \quad (30)$$

Our approximation for  $f(z)$  is to replace  $\hat{f}(z)$  by the truncation of its power series at order  $n$ . So

$$f(z) = \frac{1}{\hat{f}(1/z)} \approx \left[ \sum_{j=0}^n a_j z^{-j} \right]^{-1} \quad (31)$$

For each  $h_i$  we compute the power series of  $\hat{h}_i$  to order  $n$ . We then use them and (30) to compute the power series of  $\hat{H}_j$  to order  $n$ . Let  $1/R_j$  be the radius of convergence for the power series of  $\hat{H}_j$ . ( $R_j$  is easy to compute. It is the smallest positive number such that  $H_j(R_j)$  and  $H_j(-R_j)$  are both real.) Now consider equation (25). If  $z$  is large compared to  $R_j$ , then  $H_j(z)$  is well approximated using its hat power series. We introduce a parameter  $L > 1$  and use the

hat power series to compute  $H_j(z)$  whenever  $|z| \geq LR_j$ . When  $|z| < LR_j$ , we just use (24) to compute  $H_j(z)$ . The argument of  $H_j$  is the result of applying the previous conformal maps to 0, and so is random. Thus whether or not we can approximate a particular  $H_j$  using its hat power series depends on the randomness and on which  $z_k$  we are computing.

## 4 Choosing the parameters

Our algorithm depends on three parameters. The integer  $b$  is the number of functions in a block. The integer  $n$  is the order at which we truncate the hat power series. The real number  $L > 1$  determines when we use the hat power series approximation to the block function. These three parameters control how good our approximation is. We can compute the error that arises from using the hat power series by computing the discretized SLE curve both using the hat power series and not using them. We then define the error to be the average distance between the points on the two curves. Given some desired level of error, we want to minimize the time subject to the constraint that the error is within the desired tolerance. There is a completely different kind of error - that introduced by approximating the Brownian motion by some other stochastic process. It should converge to zero as  $N \rightarrow \infty$ . The nature of this convergence and in particular its dependence on the method of discretization is an interesting question, but we do not study it in this paper.

The behavior of our algorithm is random in that it depends on the behavior of the particular SLE sample. Since the behavior of SLE depends qualitatively on  $\kappa$ , one might expect that the behavior of our algorithm will depend significantly on  $\kappa$ . We have studied the algorithm for  $\kappa = 8/3$  and  $\kappa = 6$  and have found that the behaviors for these two values of  $\kappa$  are remarkably similar. We will restrict our discussion and our plots to the case of  $\kappa = 8/3$ , and discuss how  $\kappa = 6$  compares at the end of this section.

We continue to use the time per point (total time divided by the number of points computed) as our measure of the speed of the algorithm. For this new algorithm it is essentially independent of  $d$ , the number of time intervals between consecutive points computed, provided  $d$  is not huge. The computation of the hat power series for the conformal maps  $H_j$  does not depend on how many points we compute. When  $d$  is large enough, the time required for this computation will dominate, and the time per point will no longer be independent of  $d$ .

We first consider the effect of  $n$ . Obviously, as  $n$  grows the error should decrease and the time should increase. Figure 3 shows that as a function of  $n$ , the error is approximately proportional to  $L^{-n}$ . Figure 4 shows the growth of the time with respect to  $n$ . (In both figures we have taken  $N = 100,000$ ,  $b = 40$ , and  $L = 4$ .)

Next we consider the effect of  $L$ . As  $L$  increases we use the hat power series approximation only for larger  $z$  and so the error should decrease. However, using the approximation less frequently will increase the time required. The error decreases with  $L$  roughly as  $L^{-n}$ . (Figure 5) The dependence of the time on  $L$  shown in figure 6 is somewhat surprising. The time does not grow with  $L$  as quickly as one might expect. Eventually, as  $L$  gets large the time will be

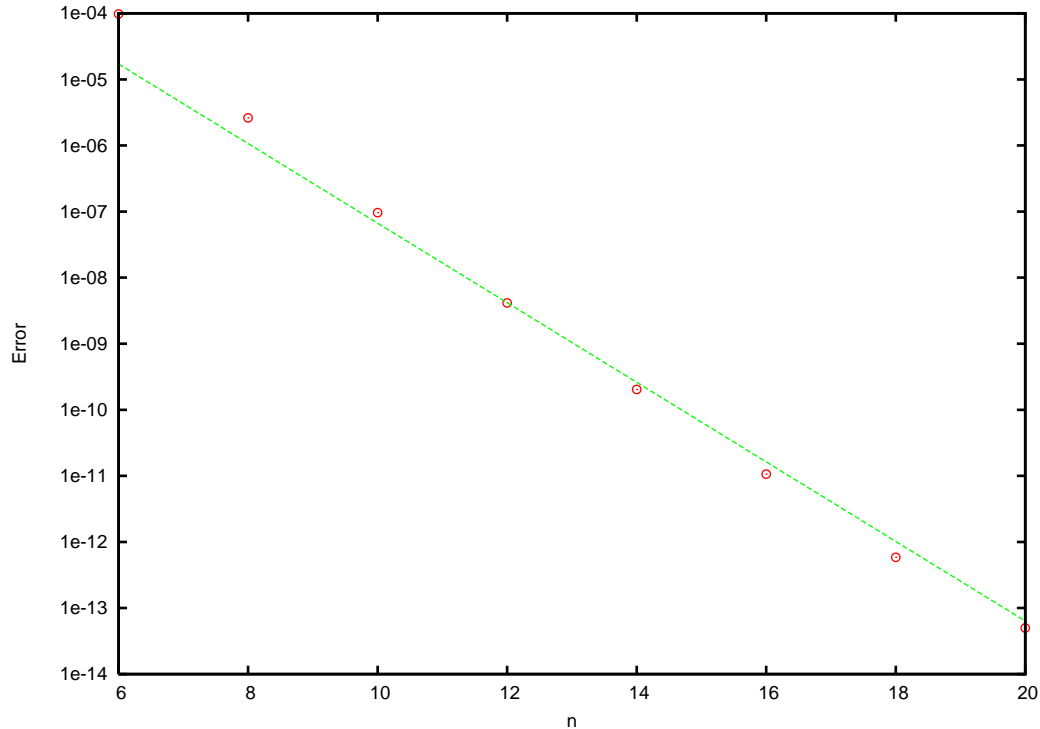


Figure 3: Error as a function of  $n$ , the order of the hat power series. The line is a fit by  $cL^{-n}$ .

on the order of the time for the standard algorithm that does not use hat power series, but this only happens at values of  $L$  considerable larger than those shown. (In both figures we have taken  $N = 100,000$ ,  $b = 40$ , and  $n = 12$ .)

Finally we consider the effect of the block size  $b$ . It is not clear a priori how the error and time will depend on  $b$ . Increasing  $b$  reduces the number of compositions to compute in (25) but it will also increase the radii of convergence  $R_j$  which will result in the hat power series approximation being used less frequently. Figure 7 shows that the error does not depend strongly on  $b$  and so  $b$  should just be chosen to minimize the time. This choice depends significantly on  $N$ . (In this figure we have taken  $N = 100,000$ ,  $n = 12$ , and  $L = 4$ .)

Figure 8 shows the time as a function of  $b$  for three values of  $N$ . (For all three curves  $n = 12$  and  $L = 4$ .) The curves have similar shapes, suggesting some sort of scaling. In figure 9 we plot the same data but now divide the time by the minimum time for that value of  $N$  and divide  $b$  by  $\sqrt{N}$ . The resulting three curves collapse nicely. This indicates that the optimal value of  $b$  is roughly proportional to  $\sqrt{N}$ . We have found that the optimal value is well approximated by  $b = 0.12\sqrt{N}$ .

We have found that the error is typically well below  $L^{-n}$ . To study which value of  $n$  is optimal we do the following. We fix a value of  $n$  and then choose  $L$  so that  $L^{-n} = 10^{-6}$ . (The choice of  $10^{-6}$  is ad hoc.) We then study the time per point as a function of  $N$ . Figure 9

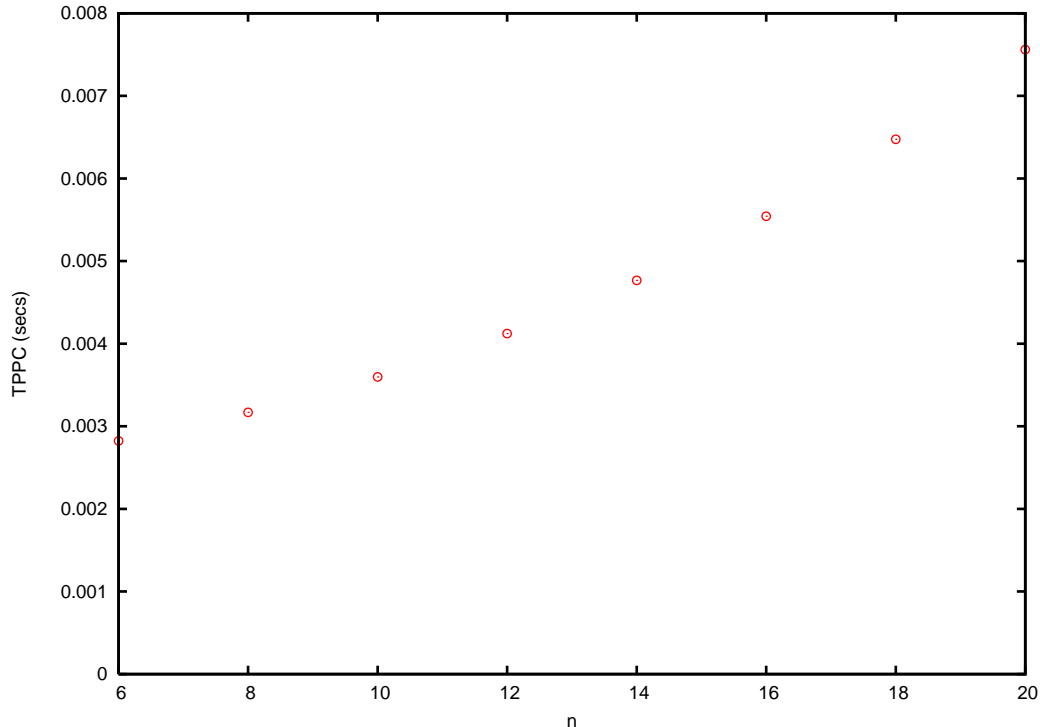


Figure 4: Time per point computed as a function of  $n$

shows the resulting plots for  $n = 8, 10, 12, 14$ . For the large values of  $N$  there is little difference between  $n = 10, 12, 14$ , but they are significantly better than  $n = 8$ .

We have carried out the same simulations and generated the same plots for  $\kappa = 6$ . Qualitatively the curves are the same. The difference between the two values of  $\kappa$  varies with the choices of the three parameters, but to a very crude approximation we have found that for  $\kappa = 6$  the algorithm is about 20% slower, and the error is about twice as large. (The error for  $\kappa = 6$  is still usually less than  $L^{-n}$ .) The optimal value of  $b$  for  $\kappa = 6$  is a bit smaller. It is better approximated by  $b = 0.1\sqrt{N}$ . The analog of figure 10 for  $\kappa = 6$  is virtually indistinguishable from the figure shown in which  $\kappa = 8/3$ . In particular, the time per point is approximately  $O(N^{0.4})$ . Taking  $n$  to be 10, 12 or 14 give similar results, all significantly better than  $n = 8$ .

## A Particular hat power series

In this appendix we give the hat power series needed for the two particular discretizations we have discussed. For the approximation that uses slits at an angle  $\alpha\pi$ , we need to compute the power series of  $\hat{h}$  where  $h(z) = (z + x_l)^{1-\alpha}(z - x_r)^\alpha$ . We have

$$\hat{h}(z) = z(1 + x_l z)^{-(1-\alpha)}(1 - x_r z)^{-\alpha} \quad (32)$$

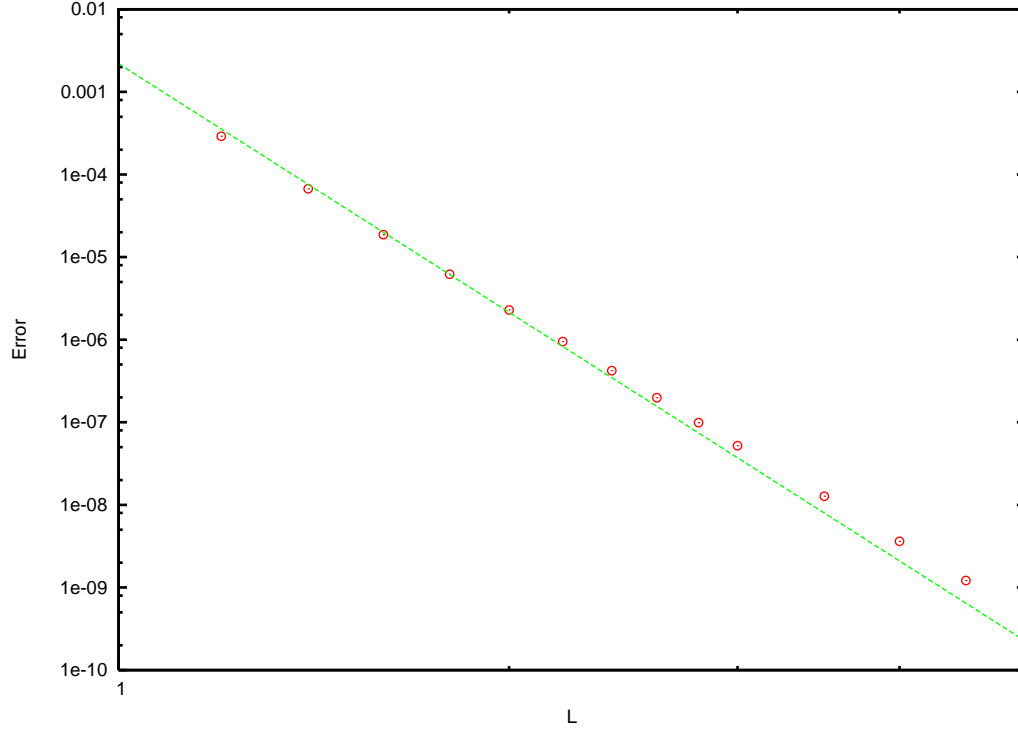


Figure 5: Error as a function of  $L$ , the parameter that determines how often we use the hat power series approximation. The line is a fit by  $cL^{-n}$ .

The power series of the last two factors are given by the formula

$$(1 - cz)^{-\alpha} = \sum_{k=0}^{\infty} \frac{\alpha(\alpha + 1) \cdots (\alpha + k - 1)}{k!} c^k z^k \quad (33)$$

For the approximation that uses vertical slits, we need to compute the hat power series of  $h(z) = \sqrt{z^2 - 4t} + x$ . First consider  $g(z) = \sqrt{z^2 - 4t}$ . We have

$$\hat{g}(z) = \frac{z}{\sqrt{1 - 4tz^2}} = z \sum_{k=0}^{\infty} \frac{1 \cdot 3 \cdot 5 \cdots (2k - 1)}{k!} 2^k t^k z^{2k} \quad (34)$$

where the power series may be obtained from (33) with  $\alpha = 1/2$ . Noting that  $h = f \circ g$  with  $f(z) = z + c$ , the hat power series of  $h$  is just the composition of the hat power series for  $f$  and  $g$ . The series for  $f$  is just

$$\hat{f}(z) = \frac{1}{1/z + c} = \frac{z}{1 + cz} = z \sum_{m=0}^{\infty} (-1)^m c^m z^m \quad (35)$$

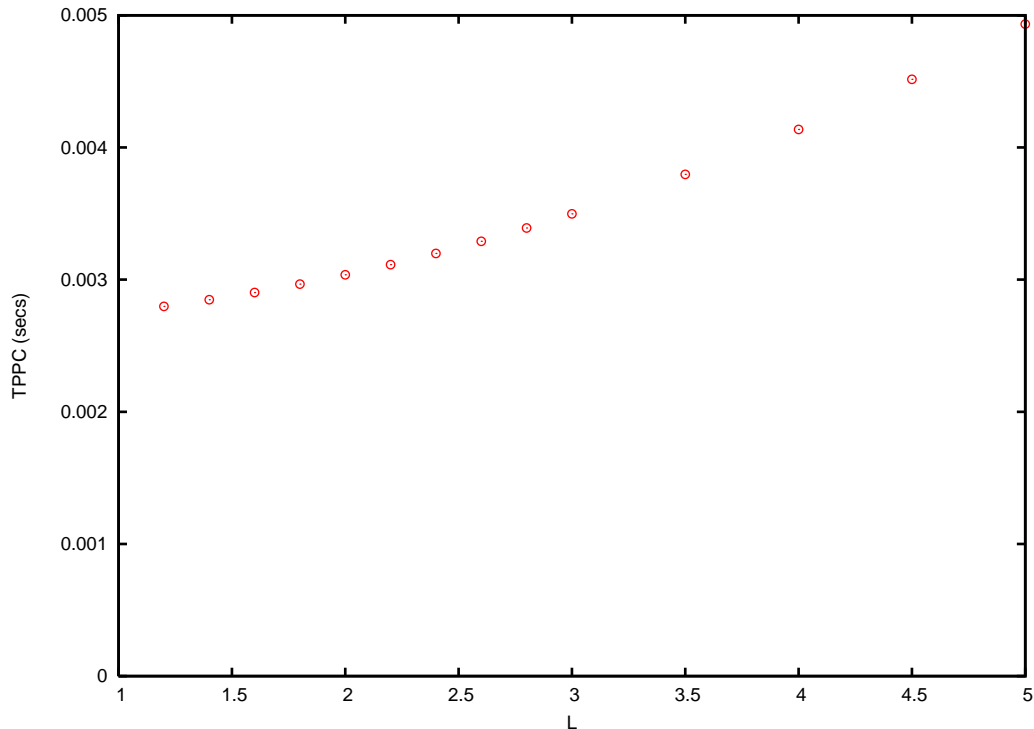


Figure 6: Time per point computed as a function of  $L$ .

**Acknowledgments:** The Banff International Research Station made possible many fruitful interactions. In particular, I learned much of the material in section 2 from conversations with Steffen Rohde and Don Marshall. This work was supported by the National Science Foundation (DMS-0201566 and DMS-0501168.)

## References

- [1] C. Amoruso, A. K. Hartman, M. B. Hastings, and M. A. Moore, Conformal invariance and SLE in two-dimensional Ising spin glasses, preprint. Archived as cond-mat/0601711 in arXiv.org.
- [2] R. Bauer, Discrete Loewner evolution, *Annales de la faculté des sciences de Toulouse Sér. 6*, **12**, 433–451 (2003). Archived as math.PR/0303119 in arXiv.org.
- [3] D. Bernard, G. Boffetta, A. Celani, and G. Falkovich, Conformal invariance in two-dimensional turbulence, *Nature Physics* **2**, 124 (2006). Archived as nlin.CD/0602017 in arXiv.org.

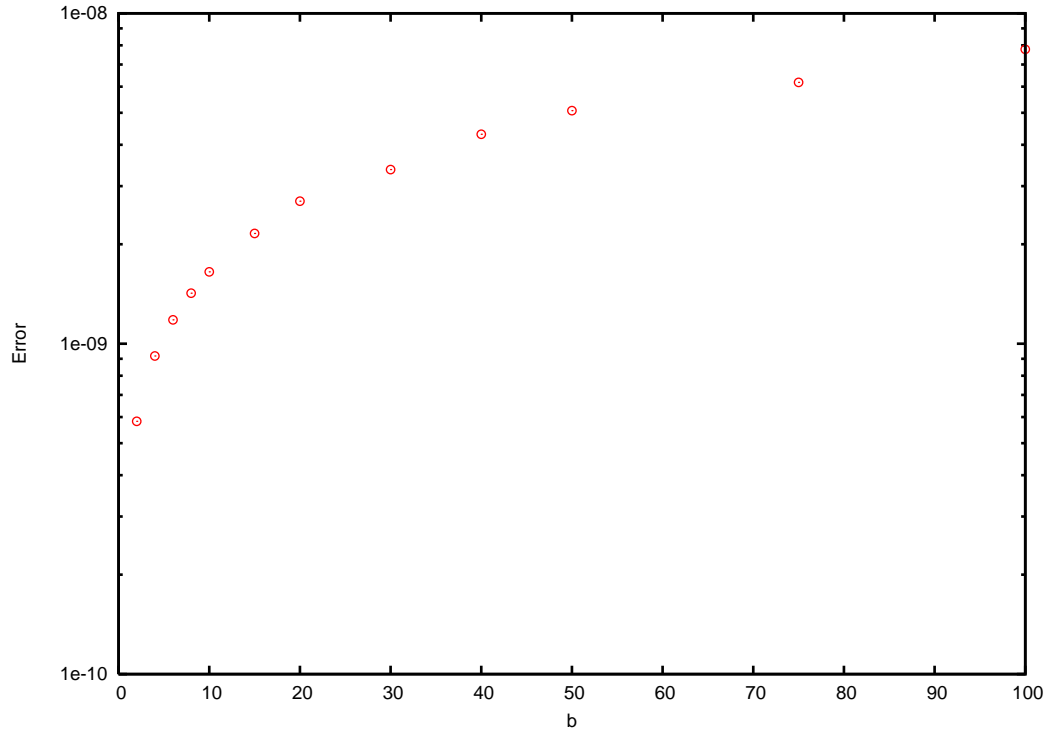


Figure 7: Error as a function of  $b$ , the number of conformal maps in a block. The data shown uses  $N = 100,000$ ,  $n = 12$ , and  $L = 4$ .

- [4] D. Bernard, G. Boffetta, A. Celani, and G. Falkovich, Inverse turbulent cascades and conformally invariant curves, preprint. Archived as nlin.CD/0609069 in arXiv.org.
- [5] D. Bernard, P. Le Doussal, and A. A. Middleton, Are domain walls in 2D spin glasses described by stochastic Loewner evolutions?, preprint. Archived as cond-mat/0611433 in arXiv.org.
- [6] T. Kennedy, Computing the Loewner driving process of random curves in the half plane, Preprint (2007). Archived as math.PR/0702071 in arXiv.org.
- [7] G. Lawler, *Conformally Invariant Processes in the Plane*, *Mathematical Surveys and Monographs*, vol. 114 American Mathematical Society, 2005.
- [8] S. Rohde, O. Schramm, Basic properties of SLE, *Ann. Math.* **161**, 879–920 (2005). Archived as math.PR/0106036 in arXiv.org.
- [9] O. Schramm, Scaling limits of loop-erased random walks and uniform spanning trees, *Israel J. Math.* **118**, 221–288 (2000).

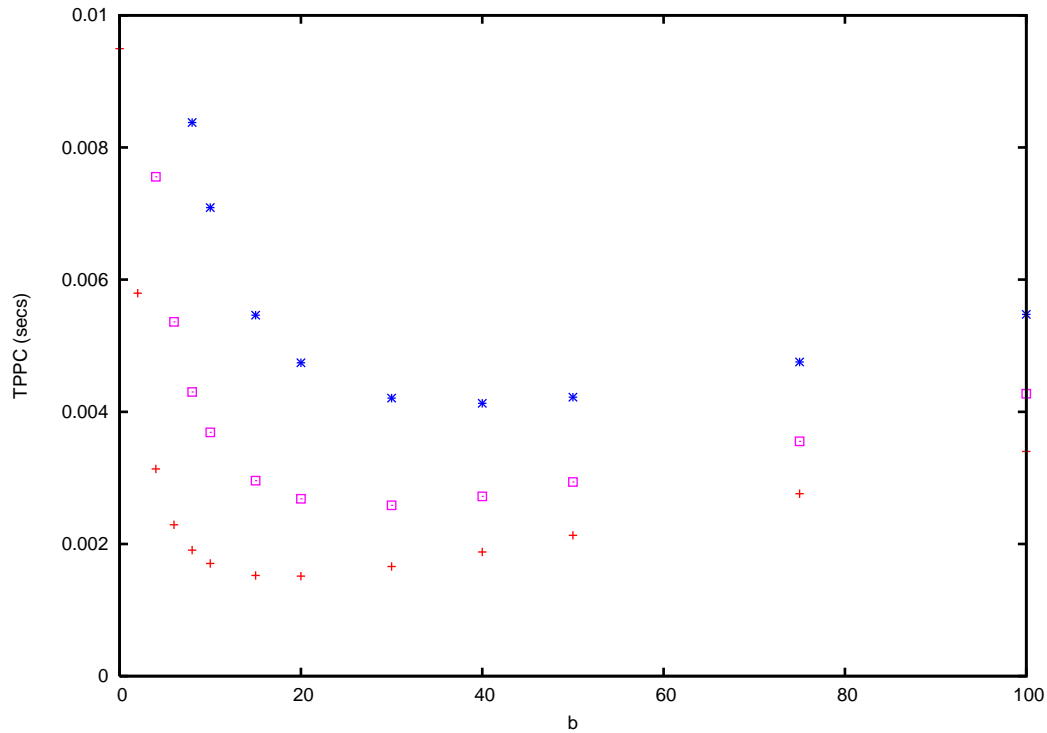


Figure 8: Time per point computed as a function of  $b$ . The three curves shown from bottom to top are  $N = 20,000$ ,  $50,000$ , and  $100,000$ .

- [10] W. Werner, Random planar curves and Schramm-Loewner evolutions, in *Lecture Notes in Mathematics, vol. 1840*, Springer Verlag, 107-195 (2004). Archived as math.PR/0303354 in arXiv.org.



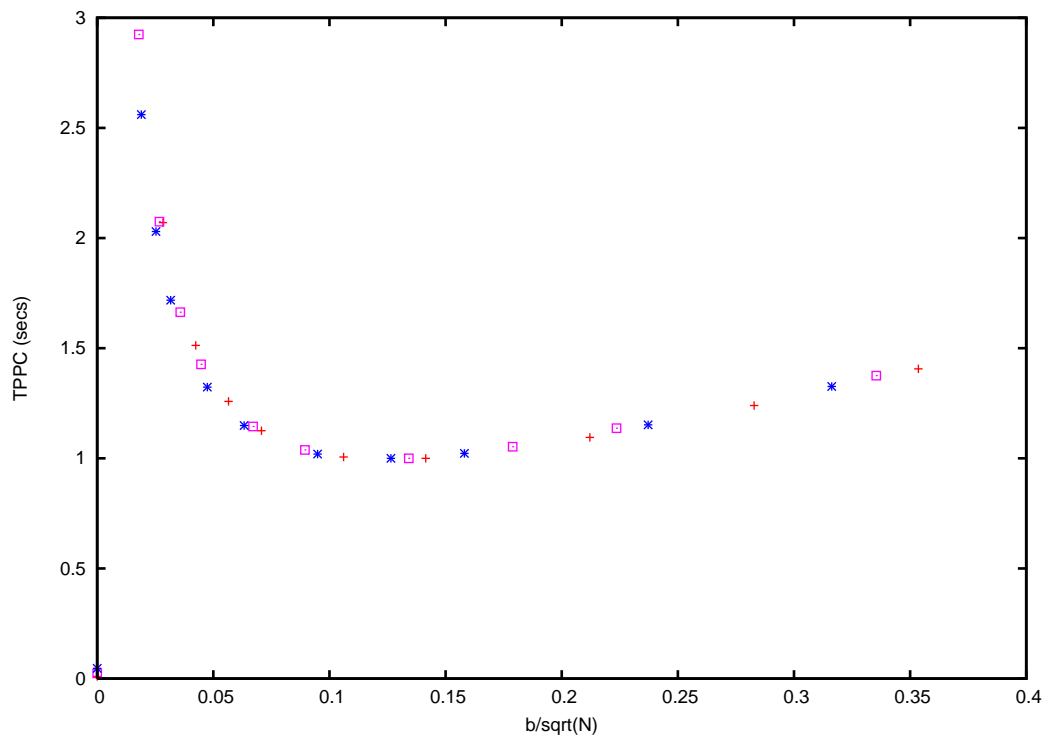


Figure 9: Scaling plot for time per point computed as a function of  $b$

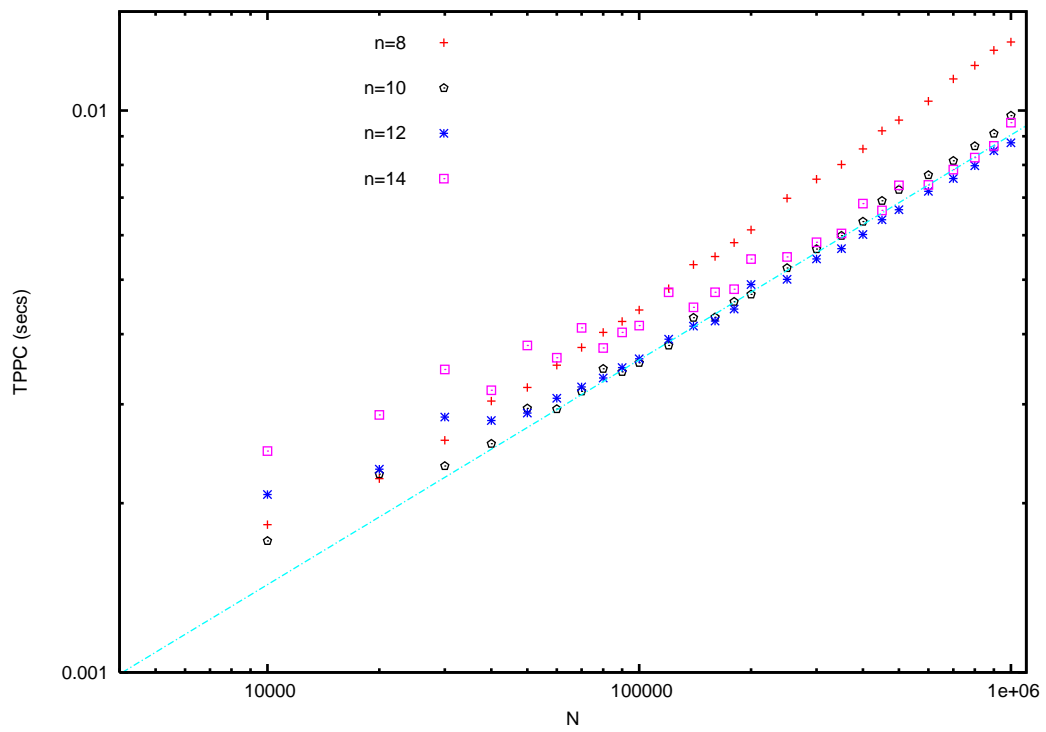


Figure 10: Time per point computed as a function of  $N$ . The four curves correspond to  $n = 8, 10, 12, 14$ . The line shown has slope 0.4.